Chaos, Solitons and Fractals 199 (2025) 116796

Contents lists available at ScienceDirect

Chaos, Solitons and Fractals

journal homepage: www.elsevier.com/locate/chaos

Effective utility-driven spatial segregation and its impact on cooperation evolution: A cultural weight-dependent perspective

Jinjin Wang [a,b], Jingjing Sun [b], Yuyou Chen [a,b,*]

[a] Center for Economic Behavior and Decision-making (CEBD), Zhejiang University of Finance and Economics, No. 18 Xueyuan Street, Xiasha Higher Education Zone, Hangzhou, 310018, Zhejiang Province, China

[b] School of Economics, Zhejiang University of Finance and Economics, No. 18 Xueyuan Street, Xiasha Higher Education Zone, Hangzhou, 310018, Zhejiang Province, China

ARTICLE INFO

Keywords:
Cultural heterogeneity
Effective utility
Spatial segregation
Boundary effect
Cultural weight

ABSTRACT

How cooperation evolves in culturally diverse populations remains a fundamental question. Individual differences in concern for others' welfare can shape social interactions, yet their role in driving large-scale social patterns is not fully understood. Here, we propose a spatial evolutionary game model where individuals possess an evolvable "cultural weight" that dictates how they value their own versus their neighbors' payoffs. We demonstrate that this utility-evaluation mechanism spontaneously drives significant spatial segregation, where like-minded individuals cluster together. This self-organized structure, in turn, powerfully influences cooperation through a "boundary effect": individuals at the interfaces of different cultural clusters exhibit significantly lower cooperation rates than those in homogeneous group interiors. Our findings reveal that subjective utility evaluation based on cultural differences is a key driver of social pattern formation, highlighting a complex feedback loop between individual culture, spatial structure, and the evolution of cooperation.

1. Introduction

The emergence and maintenance of cooperative behavior is a central issue in the evolution of both nature and human societies, attracting attention from numerous disciplines including biology, economics, and sociology. This interdisciplinary approach, often termed 'social physics', utilizes quantitative methods to understand complex social phenomena [1]. Evolutionary game theory provides a powerful theoretical framework for understanding how cooperation can arise and be sustained among populations of boundedly rational individuals under repeated interactions and selective pressures. The seminal work by Nowak and May revealed the importance of spatial structure: in spatial games, individuals only interact with their immediate neighbors, allowing cooperators to form clusters that resist invasion by defectors, a mechanism known as spatial reciprocity [2–9]. Other spatial game variants, such as spatial public goods games, explore different interaction structures and mechanisms like reputation [10].

While spatial structure is widely recognized as a key factor promoting cooperation, early models often assumed homogeneous populations. However, real-world social and biological groups often exhibit diverse forms of individual heterogeneity, for example, in behavioral tendencies, learning abilities, and resource endowments. Such heterogeneity has been shown to profoundly influence the dynamics of cooperation evolution [11–15]. In human societies, a significant source of heterogeneity is cultural heterogeneity. Culture, by shaping individuals' values, social norms, and interaction patterns, deeply affects decision-making behavior, especially the choice to cooperate in social dilemma situations [16–21].

One important aspect of how culture influences cooperative behavior is the way individuals evaluate the outcomes of social interactions, i.e., their subjective value judgments. Traditional game theory models typically assume individuals only care about their own material payoffs. However, ample research indicates that individuals' utility functions often incorporate consideration of others' payoffs, and the extent of this consideration can be modulated by cultural background [22–29]. For instance, some cultures may emphasize collective well-being more, while others prioritize individual achievement. This culturally-shaped variation in attending to others' payoffs is conceptualized in this study as a continuous "cultural weight", which regulates the trade-off an individual makes between their own interests and those of others.

* Corresponding author at: School of Economics, Zhejiang University of Finance and Economics, No. 18 Xueyuan Street, Xiasha Higher Education Zone, Hangzhou, 310018, Zhejiang Province, China.
E-mail address: chenyuyou@zufe.edu.cn (Y. Chen).

https://doi.org/10.1016/j.chaos.2025.116796
Received 27 May 2025; Received in revised form 16 June 2025; Accepted 21 June 2025
Available online 16 July 2025

When individuals with different cultural weights coexist and interact in space, complex dynamics can emerge. On one hand, differences in individuals' subjective evaluation of interaction outcomes based on their cultural weights can influence their strategy learning and behavioral imitation, thereby affecting the overall cooperation level. On the other hand, this process of interaction choice and imitation based on subjective utility evaluation can also drive the self-organization of spatial patterns, such as the clustering of individuals with similar cultural weights, a phenomenon known as spatial segregation, similar to the mechanism revealed by Schelling's model of social segregation [22,30–32], but driven by differences in utility evaluation during game interactions. This endogenously formed spatial pattern, in turn, reshapes the evolutionary path of cooperation, potentially creating unique "boundary effects" at the interfaces of groups with different cultural weights [8,33].

Based on this background, the core question of this paper is: In a spatial evolutionary game model, when an individual's attention to others' payoffs (i.e., cultural weight) is an evolvable trait that influences their evaluation of game interaction outcomes through a cultural weight-dependent effective utility, guiding their strategy and cultural weight learning updates, how does this cultural heterogeneity affect the evolution of cooperation in a spatial prisoner's dilemma game and co-emerge with spatial segregation? How do cultural weight-driven spatial patterns (such as clusters and boundaries) in turn influence the cooperative behavior of groups with different cultural weights?

To explore these questions, we construct an agent-based 2D lattice prisoner's dilemma game model. The key innovation of the model is that each agent is endowed with an evolvable cultural weight parameter, based on which a cultural weight-dependent effective utility function is defined. When updating their game strategies (cooperate or defect) and cultural weights, individuals do not solely rely on direct material payoffs but compare their accumulated effective utility with that of their neighbors. Through extensive computer simulations, we systematically analyze the behavior of a heterogeneous population with continuously variable cultural weights under different temptation to defect values. The simulation results reveal that this model mechanism can spontaneously drive significant spatial cultural segregation, that cultural heterogeneity has complex and nonlinear effects on the overall cooperation level, and that spatial segregation structures significantly influence the cooperative behavior of individuals in different locations through boundary effects. This study aims to reveal the co-evolutionary dynamics among cultural tendencies, spatial patterns, and cooperative behavior, and emphasizes that utility evaluation based on individual cultural weight differences is an important mechanism driving spatial pattern self-organization and influencing the evolution of cooperation.

The main contributions of this paper are:

- We propose a novel spatial evolutionary game model based on cultural weight-dependent utility evaluation, providing a new mechanism for studying how cultural values, by influencing subjective utility assessment, affect cooperative behavior.
- We reveal that interaction utility evaluation based on cultural weight differences is an important dynamic mechanism driving the emergence of spatial segregation patterns.
- We analyze and explain the complex nonlinear relationship and potential boundary effects existing among cultural heterogeneity, spatial segregation patterns, and cooperation levels.

The structure of this paper is as follows: Section 2 describes the model setup in detail; Section 3 introduces the simulation settings and the measurement metrics used; Section 4 presents and analyzes the main simulation results; Section 5 provides a discussion, summarizes the findings, and points out directions for future research; finally, the conclusion is presented.

2. Model

To investigate the co-evolutionary mechanism between individuals' attention to others' payoffs (quantified here as cultural weight) and cooperative behavior, we construct an agent-based spatial evolutionary game model. This model extends the classic prisoner's dilemma game framework by introducing heterogeneous, endogenously evolvable individual cultural weights, and defines cultural weight utility as the measure of individual fitness. The model's dynamic evolution follows a strictly defined sequence of time steps, achieved by simulating local interactions between individuals, utility evaluation, and strategy and cultural weight imitation updates based on utility comparison.

The model is set on an $L \times L$ two-dimensional square lattice with periodic boundary conditions (a torus). $N = L^2$ agents are distributed on the grid points. Each agent k at any time t has the following core attributes: its current strategy $S_k(t) \in \{C, D\}$, where C stands for Cooperate and D for Defect. Its intrinsic cultural weight $C_k(t) \in [0, 1]$. This is a continuous variable that quantifies the degree to which agent k values the payoff of its interaction partner when evaluating interaction outcomes. $C_k = 0$ corresponds to pure self-interested (can be seen as a manifestation of an extreme individualistic tendency), $C_k = 1$ corresponds to pure other-regarding (can be seen as a manifestation of an extreme altruistic or collectivistic tendency), and $C_k = 0.5$ represents equal concern for both parties' payoffs.

Agents only interact with their immediate spatial neighbors. This model employs the Moore neighborhood, meaning each agent interacts with its 8 surrounding neighbors (neighbors at boundaries are determined by periodic boundary conditions). This choice allows for more interaction channels compared to the simpler Von Neumann neighborhood, providing a richer local environment that can accelerate the diffusion of strategies and cultural traits.

In each time step, agents play pairwise prisoner's dilemma games with all their neighbors. The payoff matrix $\boldsymbol{\pi}$ is defined as follows: Both cooperate (C, C), both receive payoff $R = 1$. Self cooperates, opponent defects (C, D), self receives $S = 0$, opponent receives $T = b$. Self defects, opponent cooperates (D, C), self receives $T = b$, opponent receives $S = 0$. Both defect (D, D), both receive payoff $P = 0$. where $b > 1$ is the temptation to defect payoff. Let $\pi(S_k, S_l)$ denote the basic material payoff agent k receives in a single interaction with neighbor l adopting strategy S_l.

The core innovation of the model is that agents' behavioral decisions are not directly based on material payoffs π, but on their culturally-weighted utility. For a single interaction between agent k (with cultural weight C_k) and its neighbor l (with strategy S_l), the single-interaction culturally-weighted utility $U_k(S_k, S_l, C_k)$ obtained by agent k from this interaction is defined as:

$$U_k(S_k, S_l, C_k) = (1 - C_k)\pi(S_k, S_l) + C_k\pi(S_l, S_k) \tag{1}$$

This formula explicitly shows how the cultural weight C_k modulates the relative importance an individual places on their own payoff $\pi(S_k, S_l)$ and the opponent's payoff $\pi(S_l, S_k)$.

The total fitness of agent k in a complete time step t is measured by the accumulated culturally-weighted utility (Accumulated Culturally-Weighted Utility) $\mathcal{U}_k(t)$ obtained from interacting with all its neighbors. This value is calculated as the sum of single-interaction culturally-weighted utilities from agent k's interactions with all neighbors $l \in \mathcal{N}_k$ (where $\mathcal{N}_k$ is the set of agent k's neighbors) in that time step:

$$\mathcal{U}_k(t) = \sum_{l \in \mathcal{N}_k} U_k(S_k(t), S_l(t), C_k(t)) \tag{2}$$

This accumulated utility $\mathcal{U}_k(t)$ is the basis for subsequent strategy and cultural weight update decisions.

The model evolves in discrete time steps $t = 1, 2, \ldots$. Each time step t strictly follows the following 4 phases, and all agents complete the corresponding operations within each phase before proceeding to the next:

Phase 1: Calculate Utility: Each agent k according to its current strategy $S_k(t)$ and cultural weight $C_k(t)$, engages in virtual interactions with all its neighbors $l \in \mathcal{N}_k$ (whose strategies are $S_l(t)$), and according to Eq. (1) calculates the single-interaction utility for each interaction, finally according to Eq. (2) calculates and stores its accumulated culturally-weighted utility for this time step $\mathcal{U}_k(t)$.

Phase 2: Decide Strategy Update: Each agent k randomly chooses a neighbor $l \in \mathcal{N}_k$ as a reference object. It compares their accumulated utilities $\mathcal{U}_k(t)$ and $\mathcal{U}_l(t)$. The probability $P_S(k \to l)$ that agent k adopts neighbor l's strategy $S_l(t)$ is given by the Fermi rule:

$$P_S(k \to l) = \frac{1}{1 + \exp\left(-\frac{\mathcal{U}_l(t) - \mathcal{U}_k(t)}{K}\right)} \tag{3}$$

where $K \geq 0$ is the Strategy Selection Intensity parameter, controlling the influence of utility differences on the imitation probability (K smaller, selection more deterministically favors imitating the better performer; K larger, randomness is stronger).

Phase 3: Decide Culture Update: First, agent k with a preset Culture Update Attempt Probability $p_C \in [0, 1]$ decides whether to attempt to update its cultural weight. If an attempt is triggered (i.e., a random number is less than p_C), agent k again randomly chooses a neighbor $m \in \mathcal{N}_k$ as a reference object for cultural imitation. It compares their accumulated utilities $\mathcal{U}_k(t)$ and $\mathcal{U}_m(t)$. The probability $P_C(k \to m)$ that agent k adopts neighbor m's cultural weight $C_m(t)$ is also given by the Fermi rule, but using an independent Culture Selection Intensity parameter $K_C \geq 0$:

$$P_C(k \to m) = \frac{1}{1 + \exp\left(-\frac{\mathcal{U}_m(t) - \mathcal{U}_k(t)}{K_C}\right)} \tag{4}$$

If no update attempt is triggered (probability $1 - p_C$), the agent directly keeps its cultural weight $C_k(t)$ unchanged.

Phase 4: Strategy and Cultural Weight Mutation: Each agent k separately with a small strategy mutation probability $p_{s,m} \in [0, 1]$ and cultural mutation probability $p_{c,m} \in [0, 1]$ decides whether to mutate its strategy and cultural weight. If mutation is triggered, its strategy for the next time step is randomly set to Cooperate C or Defect D, and its cultural weight is reset to a new value uniformly random within the interval $[0, 1]$. At this point, a complete time step t ends, and the system enters time step $t + 1$.

This model, through the precisely defined individual cultural weight C_k and the culturally-weighted utility $\mathcal{U}_k$ based on it, couples the individual's cultural tendency (reflected in the attention to others' payoffs) with the behavioral strategy. Both strategies and cultural weights evolve through a process of social imitation based on local neighbor comparison and the Fermi rule, simultaneously the cultural weights are also subject to small-probability random mutation. This co-evolutionary process of strategy and cultural traits on a spatial structure aims to reveal how cultural factors shape macroscopic cooperation patterns at the microscopic interaction level.

3. Simulation setup and measurement metrics

In this study, we primarily focus on the steady-state behavior of the system after a long period of evolution. Each simulation runs for a total of 10,000 Monte Carlo steps (MCS). We observed that this duration is sufficient for the system to reach a dynamic equilibrium, as key macroscopic observables like the average cooperation rate stabilize well before the end of the run. Although a continuous cultural weight space theoretically allows for infinite strategic combinations, we observed that key macroscopic observables reliably converge within the specified simulation time, suggesting our setup robustly captures the system's steady-state dynamics. All presented results are obtained by averaging over the final 1,000 MCS of 1,000 independent runs for each parameter set. Simulations are conducted on square lattices of different system sizes $L \in \{10, 50, 100, 200\}$, with a total number of agents $N = L^2$. We set the strategy selection intensity parameter $K = 0.1$, cultural selection intensity parameter $K_C = 0.1$, cultural update attempt probability $p_C = 0.1$, strategy mutation probability $p_{s,m} = 0.001$, and cultural mutation probability $p_{c,m} = 0.001$. Initially, each agent's strategy (cooperate or defect) and cultural weight $C_k \in [0, 1]$ are initialized uniformly randomly within the interval $[0, 1]$.

To analyze the system behavior, we measure the following metrics:

- Average Cooperation Rate $\langle f_C \rangle$: The proportion of individuals in the system who adopt the cooperation strategy.
- Average Cultural Segregation Index $\langle S \rangle$: Used to quantify the degree of segregation formed by the clustering of individuals with similar cultural weights. For an agent k, its segregation index S_k is defined as the proportion of its neighbors belonging to the same cultural weight group as itself (e.g., classified based on $C_k < 0.5$ or $C_k \geq 0.5$). The average cultural segregation index $\langle S \rangle$ is the average of the segregation indices of all individuals.
- Susceptibility χ_O: Used to detect potential phase transition points in the system. For an order parameter O (such as average cooperation rate or average segregation index), its susceptibility is defined as:

$$\chi_O = N(\langle O^2 \rangle - \langle O \rangle^2) \tag{5}$$

  where $N = L^2$ is the total number of individuals in the system, and $\langle \cdot \rangle$ denotes the ensemble average in the steady state.
- Fraction of Boundary Agents $\langle f_{bound} \rangle$: Defined as the proportion of individuals who are adjacent to at least one neighbor from a different cultural weight group, reflecting the total length or mixing degree of the cultural weight cluster boundaries in the system. A higher value indicates a higher degree of mixing and more numerous, complex boundaries of cultural weight clusters. Conversely, a lower value indicates a lower degree of mixing and fewer, smoother boundaries of cultural weight clusters, possibly forming large homogeneous areas.
- Cooperation Rate of Boundary and Bulk Agents: The average cooperation rates are calculated separately for boundary agents and bulk agents (individuals whose neighbors are all from the same cultural weight group), used to analyze the impact of spatial structure on cooperative behavior.

4. Results

4.1. Effect of temptation to defect on overall cooperation and segregation

To investigate the impact of the temptation to defect value b on the overall cooperative behavior and spatial patterns of the system, we first measured how the average cooperation rate $\langle f_C \rangle$ and average cultural segregation index $\langle S \rangle$ change with b in the steady state. Fig. 1 shows the results for different system sizes L.

Fig. 1(a) shows the relationship between the average cooperation rate $\langle f_C \rangle$ and b. At low values of b ($b \lesssim 1.6$), the system maintains a very high level of cooperation, with $\langle f_C \rangle$ close to 1. As the value of b increases, cooperation becomes increasingly difficult, and a relatively sharp drop in the cooperation level is observed around $b \approx 1.8$. Even at very high values of b (e.g., $b > 8.0$), the cooperation rate does not completely collapse to zero but stabilizes at a significant plateau level of approximately $\langle f_C \rangle \approx 0.58$. Within the studied range of system sizes ($L = 10$ to 200), the dependence of the cooperation rate on system size L appears relatively weak. Notably, the curves for $L = 10, 50, 100$, and 200 are nearly indistinguishable in both panels. This strong consistency indicates that our main conclusions are robust and largely free of finite-size effects within this range, a finding that will be reinforced by subsequent results.

Fig. 1(b) shows the change in average cultural segregation index $\langle S \rangle$ with b. Across the entire range of b values examined, the system exhibits strong segregation formed by the clustering of individuals with

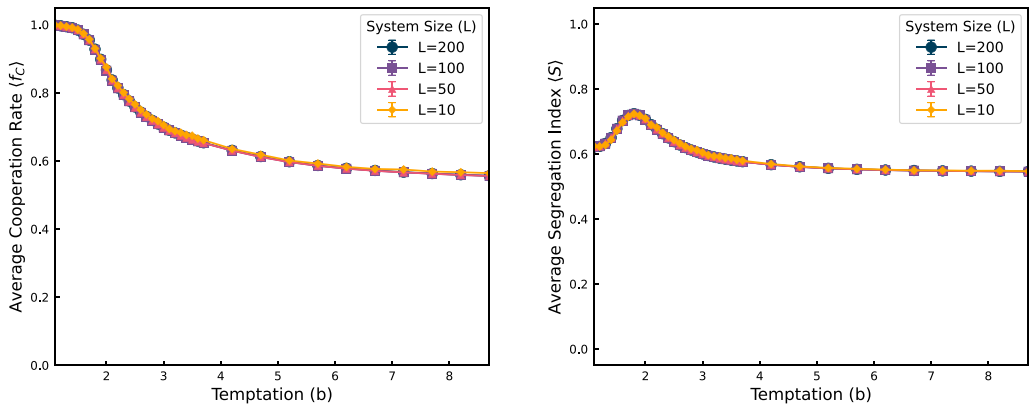

(a) Average Cooperation Rate $\langle f_C \rangle$ (b) Average Cultural Segregation Index $\langle S \rangle$

Fig. 1. Dependence of order parameters on the temptation to defect b. (a) Change in average cooperation rate $\langle f_C \rangle$; (b) Change in cultural segregation index (S). Error bars show standard error. These results reveal a complex relationship: while cooperation steadily declines with increasing temptation, the degree of cultural segregation non-monotonically peaks at an intermediate value of b.

similar cultural weights ($\langle S \rangle$ is consistently greater than 0.57). The segregation index $\langle S \rangle$ shows non-monotonic behavior with respect to b. At low b values, $\langle S \rangle$ is at a relatively high level (around 0.6). As b increases, $\langle S \rangle$ initially rises, reaching a peak (close to 0.73) around $b \approx 1.8$. When b values increase further into the low cooperation region, the segregation index $\langle S \rangle$ slightly decreases from the peak but remains at a considerably high level (around 0.57).

4.2. Susceptibility analysis

To more precisely determine the potential phase transition points in the model, we calculated the susceptibility associated with the order parameters (average cooperation rate $\langle f_C \rangle$ and average cultural segregation index $\langle S \rangle$), defined as in Eq. (5). Fig. 2 shows the relationship between the cooperation rate susceptibility χ_{f_C} (Fig. 2(a)) and the segregation index susceptibility χ_S (Fig. 2(b)) as functions of the temptation to defect b, including results for different system sizes L ($L = 10, 50, 100, 200$).

From Fig. 2(a), it can be seen that for all examined system sizes L, the cooperation rate susceptibility χ_{f_C} exhibits a significant peak around $b \approx 2.2$. The curves for different system sizes show high overlap near the peak, and the peak height shows no significant dependence on system size L. Similar to the observations in Fig. 1, the curves for different system sizes show high overlap, further confirming that our results are not dependent on the system scale.

In contrast, as shown in Fig. 2(b), the average cultural segregation index susceptibility χ_S also shows a clear peak with respect to b, but its peak location is slightly shifted towards lower b values, around $b \approx 1.5$. Similar to the cooperation rate susceptibility, the peak height of the segregation index susceptibility shows no significant dependence on system size L.

Comparing the two subfigures, it can be observed that the peak of the cooperation rate susceptibility ($b \approx 2.2$) does not exactly coincide with the peak of the segregation index susceptibility ($b \approx 1.5$), but there is a certain offset. The peak heights of both susceptibilities show no significant dependence on system size.

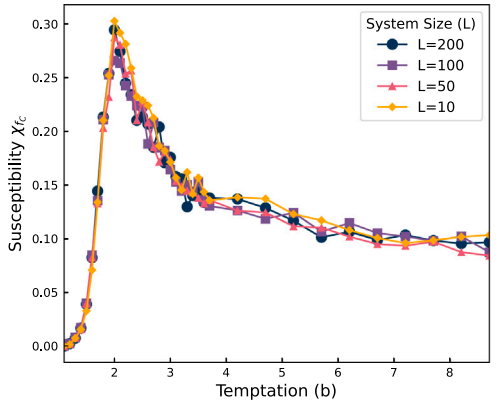

(a) Cooperation Rate Susceptibility χ_{f_C}

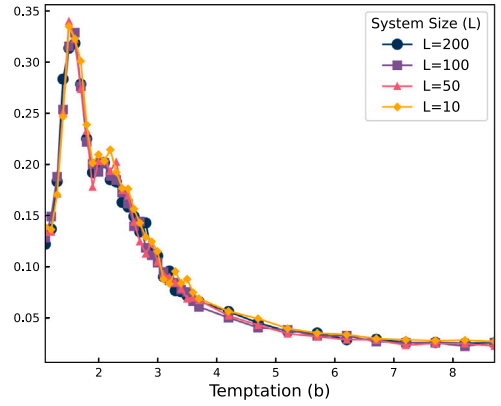

(b) Segregation Index Susceptibility χ_S

Fig. 2. Cooperation rate susceptibility χ_{f_C} (a) and segregation index susceptibility χ_S (b) as functions of the temptation to defect b, for different system sizes L. The peak of χ_{f_C} appears around $b \approx 2.2$, while the peak of χ_S appears around $b \approx 1.5$. The presence of these peaks indicates critical-like behavior, and their offset suggests that the system's spatial structure and cooperative behavior have distinct points of maximum sensitivity to the temptation to defect.

4.3. Behavioral analysis of different cultural weight groups

To gain a deeper understanding of how cultural heterogeneity, as reflected by differences in cultural weights, affects the system's behavior, we further analyzed the average cooperation rate and average cultural segregation index in the steady state for groups with different cultural weight tendencies. According to the definition of individual cultural weight C_k, we classify individuals with $C_k < 0.5$ as the self-interested group, and individuals with $C_k \geq 0.5$ as the other-regarding group. Fig. 3 shows the changes in the average cooperation rate $\langle f_C \rangle$ and average cultural segregation index $\langle S \rangle$ for these two groups as the temptation to defect b varies.

Fig. 3(a) reveals significant differences in cooperative behavior between the two cultural weight groups. The other-regarding group

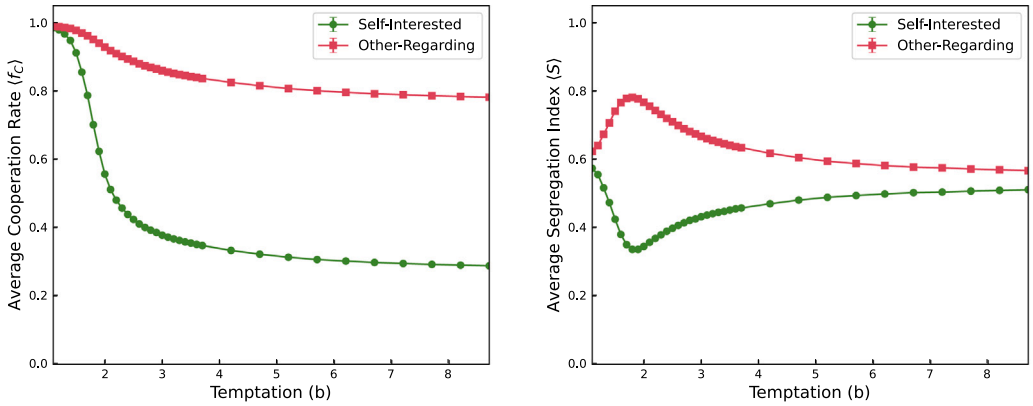

(a) Average Cooperation Rate $\langle f_C \rangle$ of Different Cultural Weight Groups

(b) Average Segregation Index $\langle S \rangle$ of Different Cultural Weight Groups

Fig. 3. Behavioral Differences between Different Cultural Weight Groups. (a) Compares the average cooperation rate $\langle f_C \rangle$ of the self-interested group ($C_k < 0.5$) and the other-regarding group ($C_k \geq 0.5$). (b) Compares their average cultural segregation index (S). The key takeaway is the profound behavioral divergence: the other-regarding group sustains high levels of cooperation and segregation, while the self-interested group is far more susceptible to defection and spatial mixing as temptation increases.

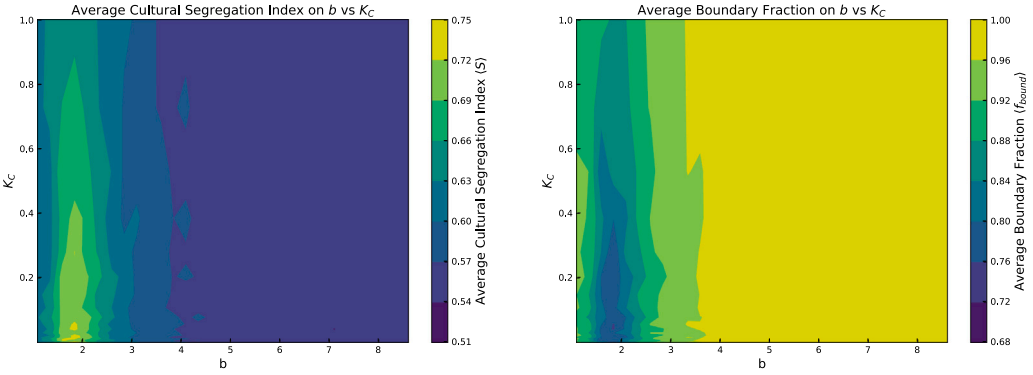

(a) Average Cultural Segregation Index $\langle S \rangle$

(b) Average Fraction of Boundary Agents $\langle f_{\text{bound}} \rangle$

Fig. 4. Steady-state spatial structure phase diagrams on the (b, K_C) parameter plane for $L = 50$. (a) Phase diagram of the average cultural segregation index (S); (b) Phase diagram of the average fraction of boundary agents $\langle f_{bound} \rangle$. These diagrams illustrate that the strongest spatial segregation (high S and low f_{bound}) occurs in a well-defined region, specifically at intermediate temptation b and high cultural selection intensity (low K_C).

(represented by red squares in the figure) consistently maintains a high average cooperation rate across the entire range of b values, decreasing slowly from nearly perfect cooperation (≈ 1.0) at low b, and still maintaining a level of about 0.78 even at high b values (e.g., $b = 9$). In contrast, the average cooperation rate of the self-interested group (represented by green circles in the figure) is more sensitive to changes in b. At low b values, its cooperation rate is close to that of the other-regarding group, but as b increases, the cooperation rate of the self-interested group drops sharply, and stabilizes after $b \gtrsim 9.0$, but the steady value (around 0.28) is much lower than that of the other-regarding group.

Fig. 3(b) shows the different performance of the two cultural weight groups in terms of spatial segregation. The average segregation index of the other-regarding group (represented by red squares in the figure) rises rapidly at low b values, peaks around $b \approx 1.8$ (about 0.77), and then declines slowly. The average segregation index of the self-interested group (represented by green circles in the figure) first decreases at low b values, reaches a minimum around $b \approx 1.8$ (about 0.33), and then rises slowly. While its segregation index remains lower than the other-regarding group's across most of the parameter space, it continues to rise at very high temptation values ($b > 8$), eventually matching it. This late-stage rise is attributed to the formation of large, homogeneous 'seas of defectors,' a different mechanism from the defensive clustering observed in the other-regarding group (see Appendix for details).

4.4. Spatial structure phase diagrams in parameter space

To systematically examine the impact of model parameters on the system's spatial structure, we calculated the steady-state average cultural segregation index $\langle S \rangle$ and the average fraction of boundary agents $\langle f_{\text{bound}} \rangle$ for different combinations of temptation to defect b and cultural selection intensity parameter K_C. The cultural selection intensity parameter K_C can be regarded here as a form of noise strength affecting the cultural evolutionary process; a larger value of K_C means lower determinism in cultural selection, i.e., weaker cultural selection intensity. Fig. 4 shows the spatial structure phase diagrams on the (K_C, b) parameter plane for a system size $L = 50$. Fig. 4(a) presents the distribution of the average cultural segregation index $\langle S \rangle$, where the color bar indicates the magnitude of $\langle S \rangle$ ranging from deep purple (low segregation) to bright yellow (high segregation). Fig. 4(b) shows the distribution of the average fraction of boundary agents $\langle f_{\text{bound}} \rangle$, where the color bar indicates the magnitude of $\langle f_{\text{bound}} \rangle$ ranging from deep purple (low boundary fraction) to bright yellow (high boundary fraction).

From Fig. 4, the complex influence of the temptation to defect b and cultural selection intensity parameter K_C on the system's spatial structure (measured by segregation index and boundary fraction) can be clearly observed. In the region of lower b values (e.g., $b < 2.5$), the segregation index $\langle S \rangle$ is relatively high, indicating noticeable spatial

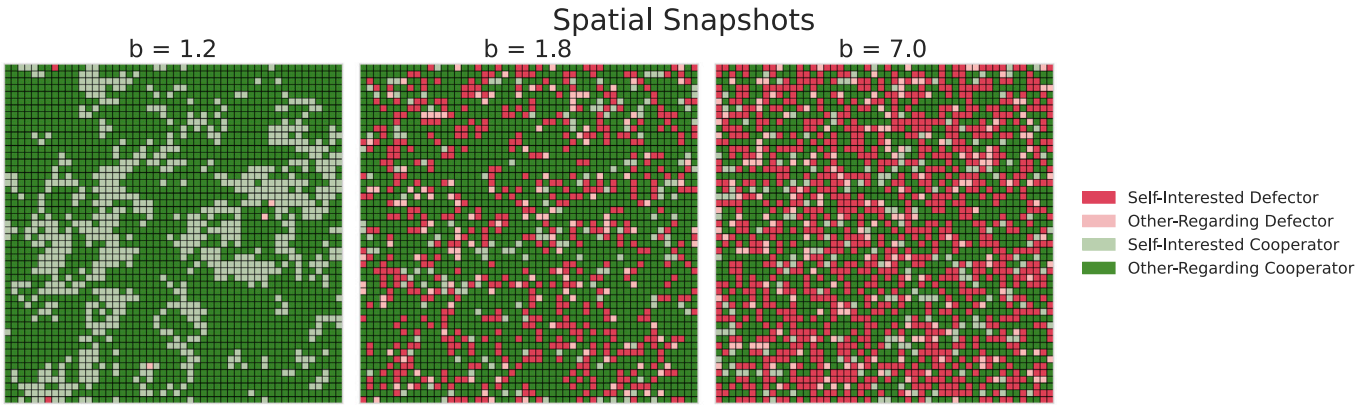

Fig. 5. Spatial snapshots of the $L = 50$ system at steady state for different temptation values b. The legend details the four agent types based on strategy and cultural weight. These snapshots visually demonstrate the system's transition across different regimes: from a cooperator-dominated state with large, homogeneous cooperator clusters at very low temptation, to a mixed state with interpenetrating clusters at intermediate temptation, and finally to a defector-dominated state with large, homogeneous defector clusters at high temptation.

segregation between cultural groups. As the value of b increases, the segregation index reaches a peak around $b \approx 1.8$, and then decreases significantly in the high b value region (e.g., $b > 3.5$). This may be related to the sharp decline in the number of cooperators under high temptation to defect, leading to reduced cultural heterogeneity. The average fraction of boundary agents $\langle f_{\text{bound}} \rangle$ is also relatively high in the lower b value region, indicating more numerous boundaries between different groups at this point. As the value of b increases, the boundary fraction decreases slightly in the intermediate b value region (approximately $2.5 < b < 4$), and increases significantly in the high b value region (e.g., $b > 4$). This is consistent with a spatial structure where cultural weight groups are highly mixed or form many small, dispersed clusters, resulting in a large total boundary length relative to the area. The influence of the cultural selection intensity parameter K_C on the spatial structure is also very important, especially in the low b value region. In the low b value region, as K_C increases (upwards along the vertical axis, cultural selection intensity weakens), the segregation index gradually decreases, indicating that moderate cultural selection intensity (i.e., lower K_C values) is conducive to the formation of spatial segregation of cultural groups. Simultaneously, in the low b value region, as K_C increases (upwards along the vertical axis, cultural selection intensity weakens), the fraction of boundary agents gradually increases, which may mean that under moderate cultural selection intensity, the groups are more compact internally, and the number of boundary agents is relatively reduced. In the high b value region, the influence of K_C is relatively weak, and the spatial structure is mainly dominated by high temptation to defect.

4.5. Spatial structure evolution at different temptation values

To visually demonstrate the effect of the temptation to defect b on the system's spatial structure, we took spatial snapshots of the $L = 50$ system at steady state for different values of b. Fig. 5 presents representative spatial distributions at $b = 1.2$, $b = 1.8$, and $b = 7.0$. The three subfigures in the figure correspond to these three temptation values from left to right. The legend explains the agent states represented by different colors: dark red indicates self-interested defectors, light pink indicates other-regarding defectors; light green indicates self-interested cooperators, and dark green indicates other-regarding cooperators. It should be noted that these snapshots are representative results from multiple simulation runs, and the actual spatial structure exhibits some randomness.

As shown in Fig. 5, at different temptation values b, the system exhibits a certain degree of spatial clustering, with individuals having similar cultural weights and strategies tending to form clusters in space. However, the scale and dominant types of these clusters vary significantly with the value of b. At a very low temptation value $b = 1.2$ (left subfigure of Fig. 5), the system is at an extremely high cooperation level, primarily occupied by cooperators, forming large, continuous cooperator regions, among which cooperators with different cultural weights (light green and dark green) are distributed. The number of defectors is very sparse, scattered sporadically, and they do not form distinct clusters. When the temptation value increases to an intermediate level $b = 1.8$ (middle subfigure of Fig. 5), the system's cooperation level decreases somewhat, and the spatial structure shows a more mixed distribution of cooperators and defectors. Individuals with similar cultural weights form mixed clusters, and self-interested defectors (dark red) significantly increase in number and begin to form some small-scale clusters. The entire space presents a dispersed, interpenetrating cluster structure. At a high temptation value $b = 7.0$ (right subfigure of Fig. 5), the system's cooperation level drops significantly, and the space is mainly occupied by defectors, forming large-scale defector clusters, with self-interested defectors (dark red) being dominant. The number of cooperators sharply decreases, making it difficult to form stable cooperator strongholds.

4.6. Spatial structure and boundary effect analysis

To quantify the degree of spatial segregation driven by cultural weight heterogeneity and to investigate how this spatial structure affects the cooperative behavior of individuals in different locations, we analyzed the proportion of boundary agents and the average cooperation rate of boundary and bulk agents. A boundary agent is defined as an individual adjacent to at least one neighbor from a different cultural weight group. Its proportion $\langle f_{bound} \rangle$ reflects the total length or mixing degree of the cultural weight cluster boundaries in the system. A bulk agent is defined as an individual whose neighbors are all from the same cultural weight group, representing an individual in a homogeneous cultural weight environment. Fig. 6 shows the change in the proportion of boundary agents with the parameter b (Fig. 6(a)) and a comparison of the cooperation rate of boundary and bulk agents in an $L = 50$ system (Fig. 6(b)).

Fig. 6(a) depicts the trend of the average fraction of boundary agents $\langle f_{bound} \rangle$ with respect to the temptation to defect b. As seen from the figure, $\langle f_{bound} \rangle$ exhibits non-monotonic behavior. In the region of lower b values (e.g., $b \lesssim 1.5$), $\langle f_{bound} \rangle$ is at a relatively high level, indicating some degree of mixing or fragmented boundaries between cultural weight groups at this point. As the value of b increases, $\langle f_{bound} \rangle$ undergoes a decrease, reaching a local minimum around $b \approx 1.8$. This may correspond to the formation of relatively clear clusters

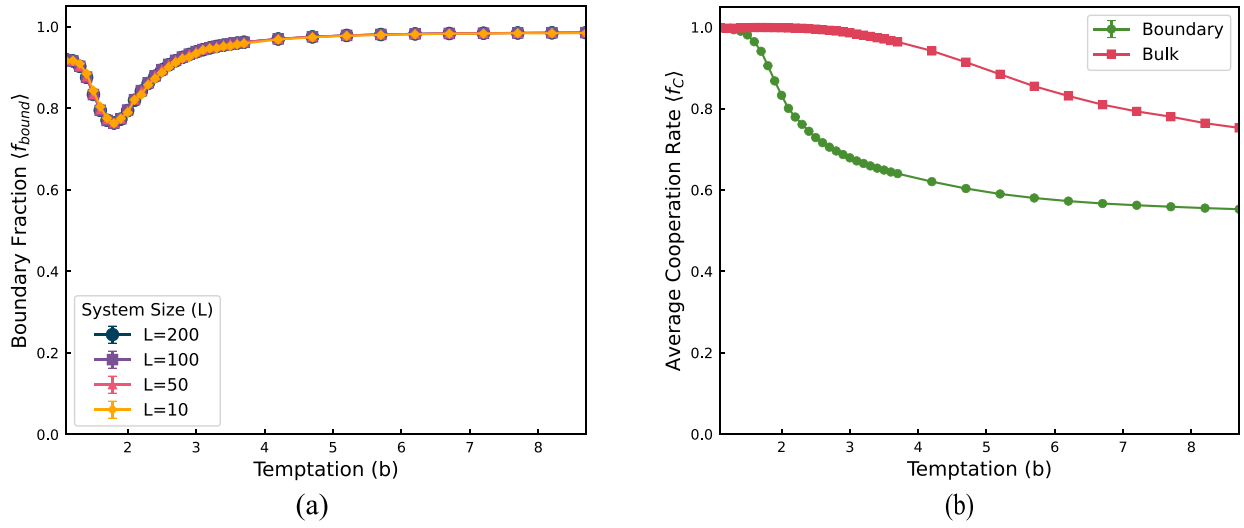

Fig. 6. Spatial Segregation and the Boundary Effect ($L = 50$). (a) The average fraction of boundary agents $\langle f_{bound} \rangle$ versus temptation b. (b) A comparison of the average cooperation rate $\langle f_C \rangle$ for boundary and bulk agents. This figure provides direct evidence for the "boundary effect": individuals at the interface of cultural groups (boundary agents) are significantly less cooperative than those within homogeneous clusters (bulk agents), especially as the temptation to defect grows.

with fewer boundaries between cultural weight groups. When b values further increase, $\langle f_{bound} \rangle$ rapidly rebounds and saturates after $b \gtrsim 4.0$, approaching 1.0. A boundary agent fraction close to 1.0 means that almost all individuals are adjacent to at least one neighbor with a different cultural weight, indicating that at high temptation values, the system forms a highly mixed or intermingled spatial structure, making it difficult for cultural weight groups to form large homogeneous areas. Data for different system sizes L show good consistency for this metric, once again indicating that this trend is robust across different system scales.

Fig. 6(b) further reveals the impact of this spatial structure on cooperative behavior, comparing the average cooperation rate of boundary and bulk agents in an $L = 50$ system. In the region of lower b values (e.g., $b \lesssim 1.5$), the average cooperation rate of both boundary and bulk agents is close to 1.0, indicating that the system is in a high cooperation state overall at this point, and the influence of spatial location on cooperative behavior is not significant. However, when b values exceed approximately 1.5, a noticeable divergence begins to appear in the cooperation rates of boundary and bulk agents. The average cooperation rate of boundary agents (green curve) drops sharply as b increases and maintains a low level in the high b value region. In contrast, the average cooperation rate of bulk agents (red curve), although also decreasing, decreases much less than that of boundary agents and remains significantly higher than the cooperation rate of boundary agents. This difference indicates that individuals located at the boundaries of cultural weight groups are more susceptible to the influence of neighbors with different cultural weights, making their cooperative behavior more easily eroded, while bulk individuals in a homogeneous cultural weight environment can maintain a higher level of cooperation more effectively. Especially in the high b value region, although the fraction of boundary agents is close to 1.0, which is consistent with a structure where cultural weight groups are highly mixed or form small, dispersed clusters, bulk agents (although their number may be reduced) can still maintain a relatively high cooperation rate. This suggests that even in an environment unfavorable to cooperation, a homogeneous cultural weight environment still provides some degree of protection for cooperation.

5. Discussion

This study systematically investigates the impact of cultural weight heterogeneity, as reflected by individual differences in attention to others' payoffs, on the evolution of cooperation and spatial structure by constructing a spatial evolutionary game model with cultural weight-dependent effective utility evaluation. Our results reveal complex interactions among cultural heterogeneity, spatial structure, and cooperative behavior.

First, our study clearly demonstrates that the cultural weight-dependent utility evaluation mechanism introduced in the model effectively drives individuals with similar cultural weights to spontaneously cluster in space, forming significant cultural segregation (Fig. 1(b), Fig. 4). This spatial segregation phenomenon is very robust across the parameter range examined and aligns with recent findings on the tendency of individuals with similar opinions or traits to cluster in social networks [22,31,32,34]. This is consistent with Schelling's classic social segregation model [30], which revealed how microscopic preferences can lead to macroscopic segregation. However, our model further shows how subjective utility evaluation based on game interaction payoffs (modulated by cultural weights) can serve as a dynamic mechanism driving this segregation, offering a new perspective for understanding the formation of communities based on values or cultural identity in real societies. Susceptibility analysis (Fig. 2) further supports the existence of critical or quasi-critical behavior related to cooperative behavior and spatial structure near specific b values. The peak of the segregation index susceptibility in Fig. 2(b) ($b \approx 1.5$) slightly precedes the peak of the cooperation rate susceptibility in Fig. 2(a) ($b \approx 2.2$). This suggests that the system's sensitivity to changes in parameter b may appear in the spatial structure dimension before the dimension of cooperative behavior. This peak offset might imply that adjustments or transitions in spatial structure to some extent precede drastic changes in the overall cooperation level, but a more definitive conclusion requires further dynamic analysis. The parameter space phase diagrams (Fig. 4) detail how the temptation to defect b and cultural selection intensity parameter K_c jointly shape this spatial segregation pattern, particularly showing that intermediate b values and moderate K_c favor the formation of the strongest spatial segregation and clear cultural weight clusters. Spatial snapshots (Fig. 5) visually demonstrate how the system transitions from cooperator-dominated clusters (low b) to a mixed state with segregated cultural weight groups (intermediate b), and finally evolves into large areas dominated by low cultural weight defectors (high b) at different b values.

Secondly, our study highlights the complex and nonlinear effect of cultural heterogeneity, as reflected by cultural weight differences, on the overall cooperation level (Fig. 1(a)). By analyzing the behavior of groups with different cultural weight tendencies (Fig. 3),

we found significant differences in cooperative behavior between the self-interested group (low C_k values) and the other-regarding group (high C_k values). While this binary classification effectively captures the primary behavioral divide, a more granular analysis presented in Appendix, which partitions agents into four distinct cultural weight groups, further confirms this finding and reveals a clear gradient in cooperative resilience. The other-regarding group, due to its intrinsically higher cultural weight, can maintain a high cooperation rate even when the game payoffs are unfavorable to cooperation (Fig. 3(a)). This aligns with observations in real life where individuals with stronger prosocial tendencies or from collectivist cultural backgrounds are more inclined to cooperate [23,24,28,35]. In contrast, the self-interested group is more sensitive to the temptation to defect b, with its cooperation rate dropping sharply at high b values. This group-level behavioral differentiation explains the trend of decreasing overall cooperation rate with increasing b. This study reveals that in systems containing cultural weight heterogeneity, groups with different cultural tendencies exhibit significantly different levels of cooperation. While this study does not directly quantify and compare with different types of homogeneous systems, the phenomenon of the other-regarding group maintaining a high cooperation rate at high b values (Fig. 3(a)), combined with existing research on how other forms of heterogeneity (such as adaptive heterogeneity or network structure heterogeneity) can promote cooperation [11–13,36,37], suggests that the impact of cultural weight heterogeneity on the overall cooperation level is complex and nonlinear. Its specific effect depends on the interaction mechanism and environmental parameters, and under certain conditions, it may differ from homogeneous systems.

More importantly, our study reveals the significant feedback effect of cultural weight heterogeneity-driven spatial structure on cooperative behavior. The spontaneously formed cultural weight segregation structure leads to a significant "boundary effect" (Fig. 6). Individuals located at the boundaries of different cultural weight clusters, being exposed to potential conflict or competition with neighbors having different cultural weights (and thus potentially different utility evaluations and behavioral patterns), face significantly increased difficulty in maintaining cooperation, leading to a substantial reduction in their cooperation rate (Fig. 6(b)). This boundary effect has been extensively studied in sociology and geography [33]. In the context of evolutionary game models, we clearly demonstrate how cultural weight heterogeneity can endogenously generate such boundaries and quantify their negative impact on cooperation [8,34]. Conversely, individuals within homogeneous cultural weight clusters can maintain a higher level of cooperation more effectively through repeated interactions with neighbors who share similar cultural weights (spatial reciprocity). This boundary effect emphasizes that in spatial systems with cultural weight heterogeneity, the maintenance of cooperation depends not only on individual strategies but is also profoundly influenced by the macroscopic spatial patterns shaped by cultural weight dynamics. The higher cooperation rate and segregation level maintained by the other-regarding group at high b values (Fig. 3(a)) may explain why the system can maintain a certain level of cooperation even when the overall cooperation rate is low. This portion of cooperation may be primarily concentrated within the homogeneous clusters formed by other-regarding individuals.

Of course, this study has some limitations. Future research could further explore the evolutionary dynamics of cultural weights themselves in more complex environments, for example, by introducing more detailed cultural transmission or learning mechanisms, or considering the adaptive expression of cultural weights in different social contexts [9,38–40]. Additionally, one could consider more complex cultural interaction rules (e.g., nonlinear utility integration methods), different network structures (such as heterogeneous networks [13,14,41]), and introducing other forms of heterogeneity (such as learning rate heterogeneity, resource heterogeneity, etc.) and their interactive effects with cultural weight heterogeneity. Mechanisms like time limitations [42] or reputation systems, as explored in spatial public goods games [10], could also be integrated into this framework to study their interplay with cultural preferences.

Furthermore, while this study focuses on cooperation in the prisoner's dilemma, the core mechanism of utility evaluation based on evolvable cultural weights holds potential for studying other prosocial behaviors. For instance, in ultimatum games, the cultural weight could modulate an individual's aversion to inequitable outcomes, impacting the evolution of fairness [43]. In trust games, it could represent an intrinsic level of trustworthiness [44]. Similarly, our framework could be adapted to explore coordination on technology adoption [45], cooperation in AI safety dilemmas [46], or open data management [47], where heterogeneous preferences and values play a crucial role. Future work could adapt our model to these diverse contexts to test the generality of our findings.

In summary, this study emphasizes the importance of considering cultural heterogeneity, as reflected by individual differences in attention to others' payoffs, and the spatial self-organization process it drives when studying the evolution of cooperation. Individual cultural weights not only influence their behavior, but can also shape the macroscopic spatial patterns, and this pattern, in turn, profoundly affects the maintenance and evolution of cooperation. Future research should further explore the complex feedback loops among culture, spatial structure, and cooperation.

6. Conclusion

This study based on evolutionary game theory and agent-based modeling, deeply explores the impact of cultural heterogeneity, as reflected by differences in individuals' attention to others' payoffs (quantified as cultural weight), on the evolution of cooperation and spatial structure in a two-dimensional spatial prisoner's dilemma game. By introducing a cultural weight-dependent effective utility evaluation mechanism, we simulated a heterogeneous system containing individuals with different cultural weights, and systematically analyzed the influence of the temptation to defect b on the system's steady-state behavior and spatial patterns. Our main research findings can be summarized as follows:

(1) Cultural Weight Heterogeneity Drives Significant Spatial Segregation: Our model mechanism can spontaneously drive individuals with similar cultural weights to cluster in space, forming homogeneous cultural weight clusters and clear cultural boundaries. This spatial segregation phenomenon is very robust across the parameter range examined, and its strength exhibits a non-monotonic dependence on the temptation to defect b, peaking around intermediate values of b.

(2) Cultural Weight Heterogeneity Has Complex Effects on Overall Cooperation Level: This study finds that in heterogeneous systems containing individuals with different cultural weights, groups with different cultural tendencies exhibit significantly different levels of cooperation, and this group-level differentiation leads to complex changes in the overall cooperation level as parameters vary due to this group-level differentiation. While this study does not directly quantify and compare with homogeneous systems, the results suggest that the impact of cultural weight heterogeneity on the overall cooperation level is complex and nonlinear, potentially differing from homogeneous systems, and that simply averaging the effects of cultural weights is insufficient to capture the complex dynamics brought about by heterogeneity.

(3) Significant Behavioral Differentiation Exists Between Different Cultural Weight Groups: The self-interested group (low C_k values) and the other-regarding group (high C_k values) exhibit

significant differences in cooperative behavior and spatial distribution. other-regarding groups tend to maintain higher cooperation rates and form stronger spatial segregation, while self-interested groups are more prone to defection, and are relatively less segregated spatially. This group-level differentiation is the basis for shaping macroscopic phenomena. The robustness of this core finding is further supported by a supplementary analysis in Appendix, which shows that while more nuanced dynamics exist, the most critical behavioral shift occurs at the threshold separating self-regarding and other-regarding tendencies.

(4) Spatial Structure Has Important Feedback Effects on Cooperation: The spontaneously formed spatial segregation structures significantly influence individual cooperative behavior through a "boundary effect". Individuals located at the boundaries of cultural weight clusters, due to facing a heterogeneous environment, exhibit significantly lower cooperation rates than individuals within homogeneous cultural weight clusters. This highlights the crucial role of spatial patterns in maintaining cooperation.

The main contributions of this study are: First, we propose a novel spatial evolutionary game model based on cultural weight-dependent utility evaluation, providing a new theoretical framework for understanding how cultural values (specifically embodied in the attention to others' payoffs) shape cooperative behavior by influencing individuals' subjective evaluation of interaction outcomes. Second, we reveal how cultural weight heterogeneity acts as an endogenous driving force, leading to significant spatial cultural segregation, and we analyze in detail how this spatial structure in turn affects the cooperative behavior of different cultural weight groups, especially highlighting the existence of the boundary effect. These findings provide important theoretical insights for understanding interactions between groups, social segregation, and cooperation and conflict in boundary regions in real societies.

In conclusion, this study emphasizes the importance of considering cultural heterogeneity, as reflected by individual differences in attention to others' payoffs, and the spatial self-organization process it drives when studying the evolution of cooperation. Individual cultural weights not only influence their behavior, but can also shape the macroscopic spatial patterns, and this pattern, in turn, profoundly affects the maintenance and evolution of cooperation. Future research should further explore the complex feedback loops among culture, spatial structure, and cooperation.

CRediT authorship contribution statement

Jinjin Wang: Funding acquisition, Validation, Writing – original draft, Writing – review & editing. **Jingjing Sun:** Validation. **Yuyou Chen:** Writing – review & editing, Writing – original draft, Validation, Supervision, Software, Conceptualization, Investigation, Methodology.

Code availability

The source code used for the simulations presented in this study is openly available at the following repository: https://github.com/chenyuyou/culture_flame2

Declaration of competing interest

The authors declare that they have no known competing financial interests or personal relationships that could have appeared to influence the work reported in this paper.

Acknowledgments

This work was supported by the Ministry of Education of the People's Republic of China Humanities and Social Sciences Youth Foundation (Grant No. 23YJCZH210).

Appendix. Supplementary information

A.1. Analysis of finer-grained cultural weight groups

In the main text, we analyzed the system by dividing agents into two broad categories: self-interested ($C_k < 0.5$) and other-regarding ($C_k \geq 0.5$). To further assess the robustness of this simplification, we conducted a more granular analysis by partitioning the agents into four distinct cultural weight groups:

- **Strongly Self-Interested (SSI)**: $0 \leq C_k < 0.25$
- **Weakly Self-Interested (WSI)**: $0.25 \leq C_k < 0.5$
- **Weakly Other-Regarding (WOR)**: $0.5 \leq C_k < 0.75$
- **Strongly Other-Regarding (SOR)**: $0.75 \leq C_k \leq 1$

We then re-evaluated the average cooperation rate ($\langle f_C \rangle$) and the average segregation index ($\langle S \rangle$) for each of these four groups as a function of the temptation to defect (b). The results are presented in Fig. A.7 .

Interpretation of results

Cooperation rate (Fig. A.7(a)): The analysis reveals a clear monotonic relationship between an agent's cultural weight and its group's cooperative behavior. As the cultural weight C increases, the cooperation rate becomes progressively higher and more resilient to the temptation to defect. While there are notable differences within the broader self-interested (SSI vs. WSI) and other-regarding (WOR vs. SOR) camps, the most significant behavioral divide remains at the $C_k = 0.5$ threshold. This confirms that the primary distinction between self-regarding and other-regarding tendencies is the key determinant of cooperative outcomes.

Segregation index (Fig. A.7(b)): The segregation dynamics are substantially more complex and non-linear. The four-group analysis reveals distinct clustering strategies:

- The Strongly Other-Regarding (SOR) group exhibits a sharp peak in segregation at intermediate $b \approx 1.8$, suggesting a strategy of forming defensive cooperative clusters when facing threats.
- In contrast, the Strongly Self-Interested (SSI) group becomes highly segregated only at very high values of b. This is likely due to a different mechanism: as high temptation turns nearly all members into defectors, they form large, homogeneous "seas of defectors", which also results in a high segregation index.
- The Weakly Other-Regarding (WOR) group's behavior contrasts with the others. Its segregation index steadily decreases as temptation b rises, indicating that this group tends to mix with other groups rather than forming distinct clusters when faced with increasing conflict.
- The Weakly Self-Interested (WSI)group consistently shows the lowest segregation, acting as a more mixed, opportunistic population.

Conclusion of supplementary analysis:

This finer-grained analysis provides deeper insights, revealing a clear gradient in cooperative resilience and multiple, distinct mechanisms driving spatial segregation. However, it also strongly validates the approach used in the main text. The most critical behavioral shift consistently occurs around $C_k = 0.5$. Therefore, the binary classification into "self-interested" and "other-regarding" groups, as used in the main text, serves as a clear and effective simplification to illustrate the core findings of our model without loss of essential explanatory power.

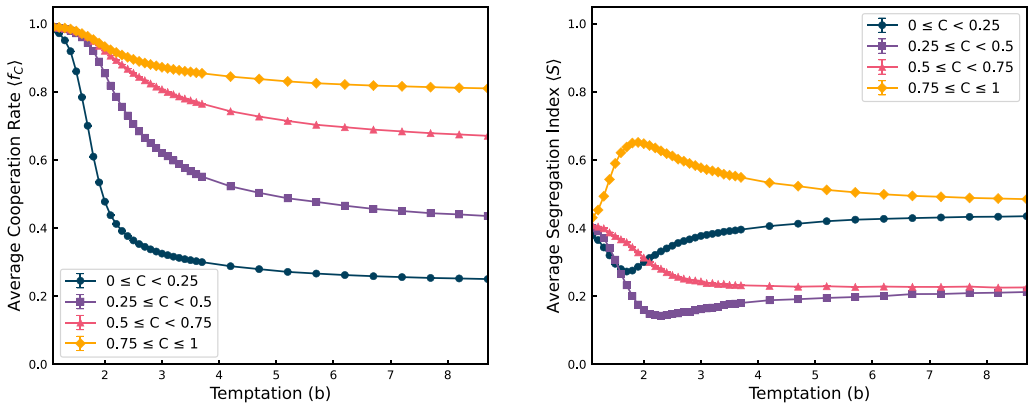

(a) Average Cooperation Rate $\langle f_C \rangle$ of Different Cultural Weight Groups

(b) Average Segregation Index $\langle S \rangle$ of Different Cultural Weight Groups

Fig. A.7. Behavioral Differences between Four Cultural Weight Groups. (a) The average cooperation rate and (b) the average cultural segregation index as a function of temptation b for the four refined groups. These results reveal more nuanced dynamics compared to the two-group analysis in the main text. This reveals a clear gradient in cooperative resilience across the groups and highlights the non-linear segregation strategies employed.

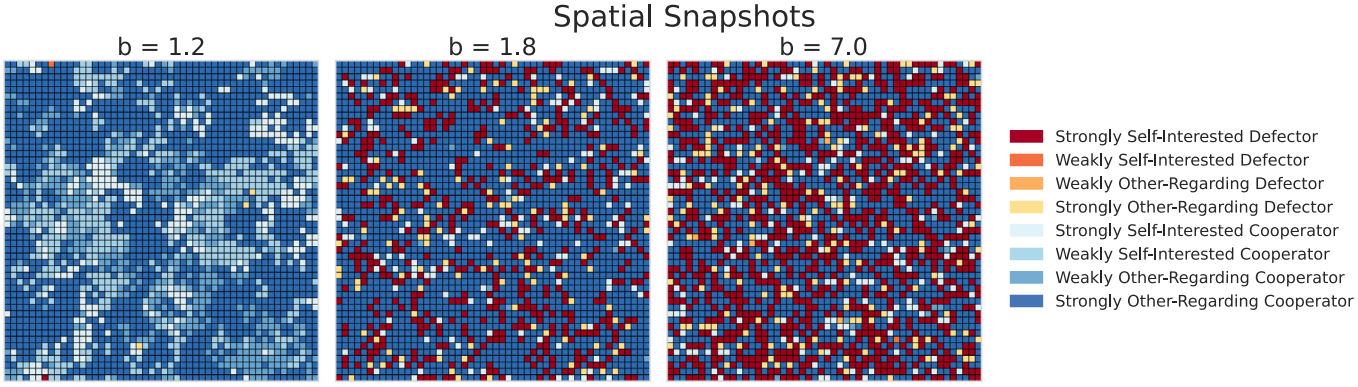

Fig. A.8. Spatial snapshots for the $L = 50$ system with four cultural groups. The panels show the steady-state spatial distribution of agents for $b = 1.2$, $b = 1.8$, and $b = 7.0$. The legend defines the eight agent types based on their cultural weight group and current strategy. These snapshots provide a visual representation of the complex spatial dynamics and segregation mechanisms at play. These snapshots visually confirm the distinct spatial dynamics, from diverse cooperator clusters at low temptation to the dominance of segregated defector 'seas' at high temptation.

A.2. Spatial snapshots with finer-grained groups

To visually complement the quantitative analysis in Appendix A.1, we present spatial snapshots of the system with agents colored according to the four refined cultural weight groups and their respective strategies (Cooperator or Defector). This results in eight unique agent types, as detailed in the legend of Fig. A.8. The snapshots are taken for three representative values of the temptation to defect, b, illustrating the evolution of spatial patterns under increasing environmental pressure.

Interpretation of spatial patterns

The detailed snapshots in Fig. A.8 reveal the distinct spatial strategies employed by different cultural subgroups:

- At low temptation ($b = 1.2$): The system exhibits a high level of cooperation, with the space predominantly occupied by various cooperator types. Strongly Other-Regarding Cooperator (dark blue) and Weakly Other-Regarding Cooperator (medium blue) form large, interconnected clusters, indicating robust cooperative networks. Weakly Self-Interested Cooperator (light blue) and Strongly Self-Interested Cooperator (lightest blue/white) are also present, often interspersed within these larger cooperative regions, suggesting their ability to cooperate under very low defection pressure. Defectors (red and orange hues) are extremely rare and scattered, appearing as isolated individuals or very small, transient groups.
- At intermediate temptation ($b = 1.8$): The spatial structure becomes significantly more fragmented and mixed. While cooperators, particularly Strongly Other-Regarding Cooperator (dark blue), still form the largest continuous regions, their dominance is challenged. Strongly Self-Interested Defector (dark red) and Weakly Self-Interested Defector (orange) have expanded considerably, forming numerous small to medium-sized clusters that interpenetrate the cooperative areas. Weakly Other-Regarding Defector (light orange/yellow) and Strongly Other-Regarding Defector (yellow) also appear more frequently, contributing to the overall mixed landscape. The boundaries between cooperative and defecting clusters are more pronounced and irregular, reflecting ongoing conflicts and adaptations.
- At high temptation ($b = 7.0$): The system is overwhelmingly dominated by defectors, forming a vast "sea" of non-cooperative agents. Strongly Self-Interested Defector (dark red) constitutes the most prevalent type, forming large, homogeneous blocks across the space. Weakly Self-Interested Defector (orange) is also widespread, often mixed with SSI defectors. Cooperation is severely diminished, with only isolated, small pockets of Strongly Other-Regarding Cooperator (dark blue) managing to persist, often surrounded by defectors. Other cooperator types (light

blue, lightest blue/white, medium blue) are almost entirely absent, indicating their inability to survive under such extreme temptation.

These visualizations provide powerful qualitative support for our findings, illustrating how micro-level cultural attributes translate into macro-level spatial organization and distinct evolutionary outcomes for different social groups.

Data availability

Data will be made available on request.

References

[1] Jusup M, Holme P, Kanazawa K, Takayasu M, Romić I, Wang Z, et al. Social physics. Phys Rep 2022;948:1–148.
[2] Nowak MA, May RM. Evolutionary games and spatial chaos. Nature 1992;359(6398):826–9.
[3] Nowak MA. Evolutionary dynamics: exploring the equations of life. Harvard University Press; 2006.
[4] Weibull JW. Evolutionary game theory. MIT Press; 1997.
[5] Smith JM. Evolution and the theory of games. In: Did darwin get it right? Essays on games, sex and evolution. Springer; 1982, p. 202–15.
[6] Perc M, Jordan JJ, Rand DG, Wang Z, Boccaletti S, Szolnoki A. Statistical physics of human cooperation. Phys Rep 2017;687:1–51.
[7] Sadekar O, Civilini A, Gómez-Gardeñes J, Latora V, Battiston F. Evolutionary game selection creates cooperative environments. Phys Rev E 2024;110(1):014306.
[8] Su Q, McAvoy A, Plotkin JB. Strategy evolution on dynamic networks. Nat Comput Sci 2023;3(9):763–76.
[9] Yang L, Jiang D, Guo F, Fu M. The state–action-reward-state–action algorithm in spatial prisoner's dilemma game. 2024, arXiv preprint arXiv:2406.17326.
[10] Flores LS, Han TA. Evolution of commitment in the spatial public goods game through institutional incentives. Appl Math Comput 2024;473:128646.
[11] Ichinose G, Saito M, Sayama H, Bersini H. Transitions between homophilic and heterophilic modes of cooperation. 2015, arXiv preprint arXiv:1506.04450.
[12] Santos FC, Santos MD, Pacheco JM. Social diversity promotes the emergence of cooperation in public goods games. Nature 2008;454(7201):213–6.
[13] Santos FC, Pacheco JM. Scale-free networks provide a unifying framework for the emergence of cooperation. Phys Rev Lett 2005;95(9):098104.
[14] Perc M, Szolnoki A. Coevolutionary games—a mini review. BioSystems 2010;99(2):109–25.
[15] Chen Y-D, Guan J-Y, Wu Z-X. Coevolutionary game dynamics with localized environmental resource feedback. Phys Rev E 2025;111(2):024305.
[16] Chen Y, Belmonte A, Griffin C. Imitation of success leads to cost of living mediated fairness in the ultimatum game. Phys A 2021;583:126328.
[17] Hofstede G. Culture's consequences: Comparing values, behaviors, institutions and organizations across nations. In: International educational and professional. 2001.
[18] Triandis HC. Individualism and collectivism. Routledge; 2018.
[19] Henrich J, Ensminger J, McElreath R, Barr A, Barrett C, Bolyanatz A, et al. Markets, religion, community size, and the evolution of fairness and punishment. Science 2010;327(5972):1480–4.
[20] Boyd R, Richerson PJ. The origin and evolution of cultures. Oxford University Press; 2005.
[21] Jeong W, Hadzibeganovic T, Yu U. Evolution of cooperation in multi-agent systems with time-varying tags, multiple strategies, and heterogeneous invasion dynamics. 2021, arXiv preprint arXiv:2104.01411.
[22] Zhong Q, Jacoby N, Tchernichovski O, Frey S. Institutional preferences in the laboratory. 2025, arXiv preprint arXiv:2502.06748.
[23] Fehr E, Schmidt KM. A theory of fairness, competition, and cooperation. Q J Econ 1999;114(3):817–68.
[24] Fehr E, Fischbacher U. The nature of human altruism. Nature 2003;425(6960):785–91.
[25] Harris LT, Fiske ST. Social groups that elicit disgust are differentially processed in mpfc. Soc Cogn Affect Neurosci 2007;2(1):45–51.
[26] Singer T, Seymour B, O'Doherty JP, Stephan KE, Dolan RJ, Frith CD. Empathic neural responses are modulated by the perceived fairness of others. Nature 2006;439(7075):466–9.
[27] Frey S, Atkisson C. A dynamic over games drives selfish agents to win–win outcomes. Proc R Soc B 2020;287(1941):20202630.
[28] Smit M, Santos FP. Learning fair cooperation in mixed-motive games with indirect reciprocity. 2024, arXiv preprint arXiv:2408.04549.
[29] Flores LS, Fernandes HC, Amaral MA, Vainstein MH. Symbiotic behaviour in the public goods game with altruistic punishment. J Theoret Biol 2021;524:110737.
[30] Schelling TC. Dynamic models of segregation. J Math Sociol 1971;1(2):143–86.
[31] Chuang Y-L, Chou T, D'Orsogna MR. A network model of immigration: Enclave formation vs. cultural integration. 2019, arXiv preprint arXiv:1901.09396.
[32] Istrate G. Stochastic stability in schelling's segregation model with markovian asynchronous update. In: International conference on cellular automata. Springer; 2018, p. 416–27.
[33] Mazzoli M, Sanchez A. Equilibria, information and frustration in heterogeneous network games with conflicting preferences. J Stat Mech Theory Exp 2017;2017(11):113403.
[34] Jia D, Dai X, Xing J, Tao P, Shi Y, Wang Z. Asymmetric interaction preference induces cooperation in human-agent hybrid game. Sci China Inf Sci 2025;68(11):1–14.
[35] Han TA, Duong MH, Perc M. Evolutionary mechanisms that promote cooperation may not promote social welfare. J R Soc Interface 2024;21(220):20240547.
[36] Cardinot M, Griffith J, O'Riordan C. A further analysis of the role of heterogeneity in coevolutionary spatial games. Phys A 2018;493:116–24.
[37] Ma Y. Optimal bias of utility function between two-layer network for the evolution of prosocial behavior in two-order game and higher-order game. 2024, arXiv preprint arXiv:2407.07119.
[38] Krakovská H, Hanel R. More than opinions: The role of values in shaping fairness and status in the ultimatum game within structured societies. 2025, arXiv preprint arXiv:2505.07060.
[39] Axelrod R. The complexity of cooperation: Agent-based models of competition and collaboration. In: The complexity of cooperation. Princeton University Press; 1997, p. 1–248.
[40] Lim IS, Capraro V. A synergy of institutional incentives and networked structures in evolutionary game dynamics of multiagent systems. IEEE Trans Circuits Syst II: Express Briefs 2021;69(6):2777–81.
[41] Capraro V, Perc M. In search of the most cooperative network. Nat Comput Sci 2024;4(4):257–8.
[42] Zhang Y, Wang J, Wen G, Guan J, Zhou S, Chen G, et al. Limitation of time promotes cooperation in structured collaboration systems. IEEE Trans Netw Sci Eng 2024.
[43] Cimpeanu T, Di Stefano A, Perret C, Han TA. Social diversity reduces the complexity and cost of fostering fairness. Chaos Solitons Fractals 2023;167:113051.
[44] Kumar A, Capraro V, Perc M. The evolution of trust and trustworthiness. J R Soc Interface 2020;17(169):20200491.
[45] Ogbo NB, Cimpeanu T, Di Stefano A, Han TA. Shake on it: The role of commitments and the evolution of coordination in networks of technology firms. In: Artificial life conference proceedings, vol. 34, Cambridge, MA 02142-1209: MIT Press One Rogers Street; 2022, USA journals-info@ mit. edu: MIT Press. 2022, p. 41.
[46] Cimpeanu T, Santos FC, Pereira LM, Lenaerts T, Han TA. Artificial intelligence development races in heterogeneous settings. Sci Rep 2022;12(1):1723.
[47] Benko TP, Pi B, Li Q, Feng M, Perc M, Vošner HB. Evolutionary games for cooperation in open data management. Appl Math Comput 2025;496:129364.